

## Research Article

**Cite this article:** Pérez-Porras FJ, Torres-Sánchez J, López-Granados F, Mesas-Carrascosa FJ (2023) Early and on-ground image-based detection of poppy (*Papaver rhoeas*) in wheat using YOLO architectures. *Weed Sci.* **71**: 50–58. doi: [10.1017/wsc.2022.64](https://doi.org/10.1017/wsc.2022.64)

Received: 28 June 2022  
Revised: 17 October 2022  
Accepted: 29 November 2022  
First published online: 15 December 2022

**Associate Editor:**

Muthukumar V. Bagavathiannan, Texas A&M University

**Keywords:**

Deep learning; open-source software; proximal sensing; SSWM

**Author for correspondence:**

Francisco J. Mesas-Carrascosa, Campus Rabanales, Department of Graphic and Geomatics Engineering of the University of Cordoba, Building C5, N-IV km. 396, 14071 Cordoba, Spain.  
Email: [ig2mecaf@uco.es](mailto:ig2mecaf@uco.es)

© The Author(s), 2022. Published by Cambridge University Press on behalf of the Weed Science Society of America. This is an Open Access article, distributed under the terms of the Creative Commons Attribution licence (<http://creativecommons.org/licenses/by/4.0/>), which permits unrestricted re-use, distribution and reproduction, provided the original article is properly cited.



# Early and on-ground image-based detection of poppy (*Papaver rhoeas*) in wheat using YOLO architectures

Fernando J. Pérez-Porras<sup>1</sup> , Jorge Torres-Sánchez<sup>2</sup> ,  
Francisca López-Granados<sup>3</sup>  and Francisco J. Mesas-Carrascosa<sup>4</sup> 

<sup>1</sup>Postdoctoral Researcher, Department of Graphic and Geomatics Engineering of the University of Cordoba, Cordoba, Spain; <sup>2</sup>Postdoctoral Researcher, imaPing Group, Plant Protection Department, Institute for Sustainable Agriculture-CSIC-Córdoba, Spain; <sup>3</sup>Research Scientist, imaPing Group, Plant Protection Department, Institute for Sustainable Agriculture-CSIC-Córdoba, Spain and <sup>4</sup>Full Professor, Department of Graphic and Geomatics Engineering of the University of Cordoba, Cordoba, Spain

**Abstract**

Poppy (also common poppy or corn poppy; *Papaver rhoeas* L., PAPRH) is one of the most harmful weeds in winter cereals. Knowing the precise and accurate location of weeds is essential for developing effective site-specific weed management (SSWM) for optimized herbicide use. Among the available tools for weed mapping, deep learning (DL) is used for its accuracy and ability to work in complex scenarios. Crops represent intricate situations for weed detection, as crop residues, occlusion of weeds, or spectral similarities between crop and weed seedlings are frequent. Timely discrimination of weeds is needed, because postemergence herbicides are used just when weeds and crops are at an early growth stage. This study addressed *P. rhoeas* early detection in wheat (*Triticum* spp.) by comparing the performance of six DL-based object-detection models focused on the “You Only Look Once” (YOLO) architecture (v3 to v5) using proximal RGB images to train the models. The models were assessed using open-source software, and evaluation offered a range of results for quality of recognition of *P. rhoeas* as well as computational capacity during the inference process. Of all the models, YOLOv5s performed best in the testing phase (75.3%, 76.2%, and 77% for F1-score, mean average precision, and accuracy, respectively). These results indicated that under real field conditions, DL-based object-detection strategies can identify *P. rhoeas* at an early stage, providing accurate information for developing SSWM.

**Introduction**

Poppy (also common poppy or corn poppy; *Papaver rhoeas* L., PAPRH) is one of the most harmful weed species regarding its infestation index in winter cereals in Spain, particularly in the Guadalquivir Valley (Andalusia, southern Spain) (Saavedra et al. 1989), and it is also the most important dicotyledonous (broadleaved) weed in Cataluña (northeastern Spain), where *P. rhoeas* can decrease wheat (*Triticum* spp.) yields up to 32% (Torra et al. 2008). This is due to biological factors related to its capacity to colonize, persist, and compete for water and light with crops. These capacities are associated with significant seed production and, as a consequence, a persistent seedbank with an extended period of germination that is the primary source of *P. rhoeas* in winter cereals (Cirujeda et al. 2006, 2008; Holm et al. 1997; Torra and Recasens 2008; Wilson et al. 1995). However, *P. rhoeas* infestations can also be related to incorrect agronomic praxis when there is no crop rotation and weed control usually consists of a single mix of postemergence herbicides sprayed from November to March, and alternation of herbicides from year to year is not a common practice (Torra et al. 2010). All these characteristics contribute to *P. rhoeas* being considered a difficult to control weed. This situation is becoming worse due to herbicide-resistant biotypes, especially in mono-cereal crop systems, together with the reduction of tillage practices to reduce costs and soil degradation and consequently greater herbicide dependence (Cirujeda et al. 2001; Torra et al. 2010).

Traditionally, weed management has been addressed through the application of control measures to the entire field crop. However, management programs, including herbicide use, can be optimized by targeting weed-infested areas and not treating weed-free areas (Heijting et al. 2007; Izquierdo et al. 2009, 2020; Jurado-Expósito et al. 2003). This is the basis of site-specific weed management (SSWM), which involves weed control measures only where and when they are truly needed, that is, rational weed management within a crop field to match the variation in location, density, and composition of the weed population (Fernández-Quintanilla et al. 2020). One of the crucial components for SSWM is to provide accurate and timely postemergence control based on early weed infestation maps to reduce the competition between weeds and crop in the early growth

phases. Remote or proximal (on-ground) sensing technologies are able to capture information that, once processed and analyzed, can be used to detect and classify weeds and crop and provide maps on which an SSWM strategy can be based, as reviewed by several authors (Fernández-Quintanilla et al. 2018; López-Granados 2011; Mulla 2013; Peteinatos et al. 2014).

In relation to remote sensing, reliable information has been published about imagery acquired by unmanned aerial vehicles (UAVs) to provide accurate and early weed infestation maps at the field scale in vineyard and wide-row crops (e.g., sunflower (*Helianthus annuus* L.), cotton (*Gossypium hirsutum* L.), and maize (*Zea mays* L.), which are usually sown 70 cm apart), providing significant herbicide savings (Jiménez-Brenes et al. 2019; López-Granados et al. 2016; Peña et al. 2015; Pérez-Ortiz et al. 2016). These authors emphasized that crop and weed plants at the early phenological stage (4 to 6 leaves unfolded, Biologische Bundesanstalt, Bundessortenamt, and Chemical industry scale [BBCH] scale; Meier 2001) generally have similar color, appearance, and reflectance characteristics and that the distribution of weeds can be as isolated plants or in small patches, indicating the necessity to work with very high spatial resolution imagery, as is generated by UAVs (<5-cm pixels). However, for narrow-row crops such as winter cereals (e.g., wheat or barley (*Hordeum* spp.)) usually sown in rows 15 cm apart, an additional difficulty arose for generating accurate orthomosaicked UAV imagery in which the crop rows must be correctly aligned (Gómez-Candón et al. 2014; Mesas-Carrascosa et al. 2015) for the first discrimination of bare soil and vegetation fraction (Torres-Sánchez et al. 2014, 2015). According to that, and taking into account that weeds grow mixed with crop plants, early *P. rhoeas* identification in winter cereals is challenging as *P. rhoeas* must be detected when cereal crop plants do not cover the soil (to avoid the complete occlusion of weeds by the crop) and due to the very small size of *P. rhoeas* plants (2 to 4 leaves unfolded, BBCH scale; Meier 2001) at the time when weed control (e.g., herbicide application) is recommended. Detection of *P. rhoeas* has been addressed by Peña-Barragán et al. (2017) using UAVs flying at 30-m altitude and images with 0.60 cm pixel<sup>-1</sup> of spatial resolution, achieving good discrimination between bare soil and wheat but limited accuracy in weed detection. Additionally, Pflanz et al. (2018) and de Camargo et al. (2021) detected *P. rhoeas* in a more advanced growth stage using a UAV flying at 1 to 6 m over the ground.

One potential alternative is to use on-ground imagery of the winter cereal under field conditions, as this imagery allows millimeter resolution. However, to our knowledge, there are only a few papers supporting the objective of early weed detection in winter cereals. Tellaeche et al. (2011) discriminated between avena (*Avena sterilis* L.) and wheat plants at early growth phases by using an automatic computer vision system involving image segmentation and decision making. Pérez et al. (2000) detected broadleaved weeds in cereal crops by analyzing RGB imagery and detected weeds by locating plant material between rows of a small grain cereal crop in images recorded in video format. Andújar et al. (2012) used an ultrasonic sensor in a wheat field infested by grass and broadleaved weeds and found that sensor readings were well correlated with weed density and coverage. However, there are not yet any studies reported about the use of proximal sensing for the early and timely detection of *P. rhoeas* in winter cereals to provide further development of an SSWM strategy. This objective could be achieved by improved and more powerful and efficient computer capacity together with advances in graphical processing units (GPUs) for accurately processing a large volume of data in a short time.

Different image processing techniques have been applied for weed and crop classification (Hemming and Rath 2002; Woebbecke et al. 1995). The main challenge is that both crops and weeds can have similar visual characteristics like color or texture. Thus, by extracting shape, color, and texture features (Kazmi et al. 2015; Meyer et al. 1998), it is possible to identify weeds and crops. However, weed identification faces issues with respect to lighting; image resolution; soil type; and small variations between weeds and crops in terms of shape, texture, color, and position (i.e., overlapping) (Dyrmann et al. 2016). The use of deep learning (DL) models for weed classification and detection offers a new framework capable of successfully dealing with the particularities of early-season weed detection. Depending on how training and validation data are labeled, DL methods are classified as supervised, unsupervised, and semi-supervised (Hasan et al. 2021). Supervised DL methods, in which training and validation data sets are manually labeled, are being used by most studies to detect and classify weeds in crops (Khan et al. 2021; Sharpe et al. 2020). Unsupervised methods are those in which the training data set is not labeled. These unsupervised methods, although used less often, can achieve good-quality weed discrimination, reducing the time costs of manual data labeling (dos Santos Ferreira et al. 2019). Finally, semi-supervised methods take the middle ground between supervised and unsupervised learning (Shorewala et al. 2021). Su et al. (2021) proposed a real-time segmentation of interrow rigid ryegrass (*Lolium rigidum* Gaudin) weed plants in wheat using on-ground sensing. The performance of different DL techniques has been recently reviewed for detecting, localizing, and classifying a wide range of broadleaved and grass weed species in an extensive set of herbaceous crops, including wide- and narrow-row crops, using proximal and remote images (Hasan et al. 2021). Among the existing DL models, the “You Only Look Once” (YOLO) architecture stands out, because of its fast inference and high accuracy, and it is also able to calculate and predict all feature images at the same time (Thuan 2021). YOLO is an end-to-end DL-based detection model that determines the bounding boxes of the objects present in the image and classifies them in a single pass. Thus, although there are two-stage models, these are not effective for application in the detection of vegetation (crops or weeds), mainly due to their slow detection speed (Jin et al. 2022). In addition, YOLO models use a combination of HSV (hue, saturation, value) color space modification and classical methods (rotation, translation, scale, shear, perspective, flip, mosaic, or blending, among others) for data augmentation. Therefore, this increase in the variability of data enables an improvement of the results (Perez and Wang 2017). Since the first publication of YOLO (Redmon et al. 2016), five versions of this DL model have appeared, each including new features (Thuan 2021). Among these versions, modified architectures of YOLOv3 and YOLOv4 have been successfully applied for weed detection in different wide-row crops (Czymbek et al. 2019; Gao et al. 2020; Partel et al. 2019; Ying et al. 2021). Despite all this work, no one has reported using YOLO for *P. rhoeas* discrimination in winter cereals.

The main motivation for the present study is to evaluate if it is possible to detect *P. rhoeas* at the early stage, which involves small object detection in a field-scale scenario (real world). In this context, the objective of this work was to assess the accuracy and inference speed of different YOLO versions (from v3 to v5) for early *P. rhoeas* detection in proximal RGB images acquired in a wheat field. To the best of the authors' knowledge, this is the first time that YOLOv5 has been proposed for weed detection.

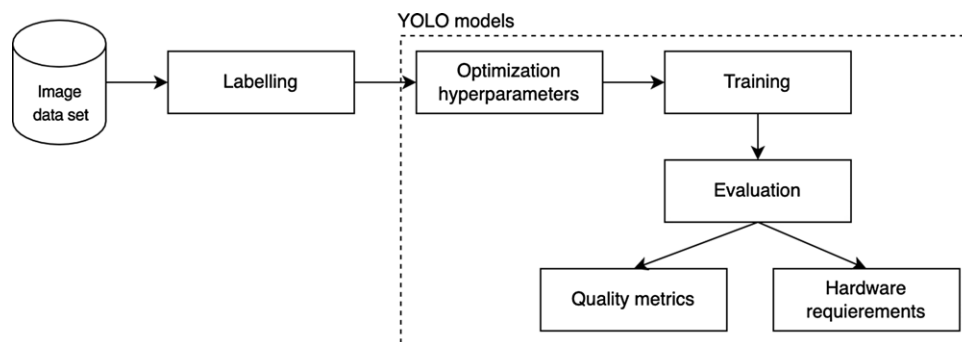


**Figure 1.** Flowchart used for *Papaver rhoeas* detection.



**Figure 2.** Example of *Papaver rhoeas* in wheat, both at growth stages 12 to 14 of the BBCH scale. The upper right image includes a Euro coin as a reference to the plant's small size.

## Materials and Methods

Figure 1 summarizes the process carried out to detect *P. rhoeas* in wheat at an early stage under real field conditions using proximal RGB sensors. First, the data acquisition and subsequent data annotation for each weed plant were carried out. Six object-detection models based on different YOLO architectures were studied due to their strong feature-learning capabilities. Each DL model was evaluated considering object-detection quality and performance in terms of hardware requirements. Quality was evaluated through precision, recall, F1-score, mean average precision (@mAP.5), and accuracy metrics, whereas GPU and central processing unit (CPU) capabilities were analyzed to determine the most efficient model in the inference phase.

### Data Collection

In this study, images were acquired at noon from a commercial winter wheat cereal plot located at Artesa de Segre, Spain (41.908572°N, 1.012275°E, WGS-84). Due to the importance of weed identification at the early growth stage, images were registered at growth stages 12 to 14 BBCH scale (Meier 2001), corresponding to the 2 to 4 leaves unfolded and considering different situations. As an example, as shown in Figure 2, *P. rhoeas* appeared isolated (Figure 2, no. 4) or partially hidden by the crop (Figure 2, no. 2), together with crop residues (Figure 2, no. 3), or on soil with different tonalities (Figure 2, nos. 1 and 4) and plant densities, thus providing a robust data set including all possible situations to be

considered in weed detection. Images were recorded with a Sony FDR-AX100E (Sony Corporation, Tokyo, Japan), which is an RGB (red, green, blue) sensor, registering images at approximately 1.5-m height above ground level with a focal length equal to 9 mm. The sensor size had dimensions equal to 13.2 by 8.8 mm and a resolution of 14.2 megapixels. This sensor configuration and the image acquisition height resulted in a ground sample distance of approximately 0.5 mm.

One of the challenges of detecting weeds is the low detection accuracy caused by their small size (Oh et al. 2020). In this context, a small object-detection task in computer vision is one in which the size of the object is less than or equal to 32 by 32 pixels in an image of 640 by 640 pixels (Tong et al. 2020). In the present study, registered RGB images have dimensions equal to 5,024 by 2,824 pixels, while *P. rhoeas* ranges from 18 by 18 to 5 by 5, which makes it classifiable as a small object-detection task. Because the object-detection model requires RGB images with dimensions equal to 416 by 416 pixels as input, the original images need to be automatically resized by the detection algorithm. However, being at the seedling growth stage, the *P. rhoeas* plants were very small, so a significant loss of information would be generated in this resampling process. Therefore, to work with the images at full spatial resolution, we cropped them to 416 by 416 pixels using OpenCV (Open Source Computer Vision Library; OpenCV 2021), which resulted in a new image data set in which each individual RGB image was cropped into 82 individual images. These smaller image sizes allowed faster identification (Jiang et al. 2022),

and maintaining the spatial resolution ensured no information was lost during the training process. Subsequently, the cropped images were mosaicked back to the original size of the input image. In this study, 77 images were cropped to 416 by 416 pixels, resulting in a data set of 6,319 images.

### Object-Detection Algorithms

Among all YOLO architecture versions, the following models and levels were analyzed: YOLOv3, Scaled-YOLOv4 (YOLOv4-CSP and YOLOv4-P5 levels), and YOLOv5 (YOLOv5-s, YOLOv5-m, and YOLOv5-l). Although both YOLOv4-P7 and YOLOv4-P9 have deeper neural networks, they could not be evaluated due to limited available memory of the computer. In addition, previous YOLO architectures were not considered, as they reuse classifiers or locators to perform detection, while YOLOv3 in 2018 was the first version to divide the image into regions and predict the bounding boxes and weighted probabilities of each region (Redmon and Farhadi 2018). Thus, YOLOv3 changed the softmax classifier into an independent logistic regression classifier, offering a fast processing neural network with 30 images or frames per second (FPS) and a @mAP.5 of 57.9% on the Microsoft COCO database (Redmon and Farhadi 2018). In addition, predictions on YOLOv3 are made on the whole image and not by region, allowing it to be based on a global context. However, YOLOv3 showed problems with multiscale features, and Scaled-YOLOv4 was subsequently developed in 2020. It is a lightweight version of YOLOv3 that reduces the requirements of equipment, offering an accuracy on the Microsoft COCO data set equal to 55.8% (Bochkovskiy et al. 2020) with the best speed-to-precision ratios, ranging from 15 FPS to 1,774 FPS. In addition, Scaled-YOLOv4 is an improvement over YOLOv3 with the inclusion of cross stage partial (CSP) (Wang et al. 2020), which allows cross networks to be increased by augmenting the scaling. To date, YOLOv5, published in 2020 (Jocher et al. 2020), is the latest version of YOLO. It adds unique focus and bottleneck CSP modules to improve and merge image features to resolve the problem of missed and mischecked multiscale feature target detection.

### Training Data Set Labeling

Because YOLO architecture is a supervised learning method, it requires manual labeling on images to learn by itself throughout the regions of interest (ROIs) definition. In addition, it also needs to manually define ROIs for the testing set to evaluate the quality of the model. Therefore, to train the models previously, ROIs in the images were manually delimited using the open-source image data annotation software Label Studio (<https://github.com/heartexlabs/labelimg>). Because our experiment relies on the accurate labeling of *P. rhoeas* class in the image data set, a group of three experts with expertise in weeds carried out the labeling of the data set. First, one expert performed preliminary labeling work on the data set. Then, another expert checked the annotations and corrected possible mislabeling. The third expert checked all the annotation work to ensure the consistency of the results. From the image data set, a total of 11,170 *P. rhoeas* samples were marked, taking into account different criteria. First, each ROI should cover as little background as possible. In addition, ROIs should consider that *P. rhoeas* could be in different situations: (1) isolated, (2) partially hidden (occluded) by the crop, (3) together with crop residues, and (4) with soil as background showing different tonalities. Subsequently, the samples were divided into three groups, with 70% used for training, 20% for testing, and 10% for validating the model.

**Table 1.** Definition of evaluation parameters.

Parameter	Definition
True positive (TP)	<i>Papaver rhoeas</i> object considered as <i>P. rhoeas</i>
True negative (TN)	No- <i>P. rhoeas</i> object considered as no- <i>P. rhoeas</i>
False positive (FP)	No- <i>P. rhoeas</i> object considered as <i>P. rhoeas</i>
False negative (FN)	<i>P. rhoeas</i> object considered as no- <i>P. rhoeas</i>
Precision (P)	TP/(TP + FP)
Recall (R)	TP/(TP + FN)
F1-score	$2 \times (\text{precision} \times \text{recall}) / (\text{precision} + \text{recall})$
Accuracy	(TP + TN)/(TP + FP + TN + FN)
Mean average precision (@mAP.5)	$1/N \times \sum_{i=1}^N AP_i$ , where $AP = \int_0^1 P(R) dR$

### Model Parameter Selection

The training was carried out on the Google Colab Pro service with a 16-GB Tesla P100 GPU and 16 GB RAM. To increase the accuracy for *P. rhoeas* detection, the six YOLO architectures were trained on the *P. rhoeas* data set. The newly learned features were coupled with pretrained weights of the COCO network with the help of transfer learning.

Thus, the hyperparameters for the six YOLO architectures were optimized, and the initial weights provided by the authors of the architectures for the pretrained COCO network were used. However, the batch size selected for training depended on the YOLO architecture, with a value equal to 32 for YOLOv3 and YOLOv4 and 64 for YOLOv5 used. Finally, each model was trained up to 500 epochs, taking into account that learning converged properly (Oppenheim et al. 2019).

### Evaluation

First, for the assessment of the *P. rhoeas* object-detection model considering each architecture and according to a combination of the true and predicted labels, true positives (TP), true negatives (TN), false positives (FP), and false negatives (FN) were counted to calculate the precision, recall, F1-score, @mAP.5, and accuracy metrics based on the definitions presented in Table 1.

Second, we evaluated which of the six YOLO architectures was the most efficient in terms of the use of computational resources. This was assessed by determining the percentage of GPU usage, the number of epochs per second analyzed in training, and the FPS inferred using both GPU and CPU in testing.

### Results and Discussion

The optimized hyperparameters for YOLO architectures 3, 4, and 5 are shown in Table 2. These results were obtained taking into account 300 iterations every 15 epochs and using as initial weights those provided by the authors of YOLO from the pretraining of the COCO network. Subsequently, each model was trained for 500 epochs to guarantee learning convergence by using these optimized hyperparameters.

Table 3 shows the precision, recall, F1-score, @mAP.5, and accuracy values obtained in the testing phase for *P. rhoeas* detection. Both YOLOv4 versions presented the lowest values in precision, below 70%, while YOLOv3 and the three YOLOv5 architectures exceeded this value. Of these, YOLOv3 achieved the highest precision (78.6%), followed by YOLOv5l and -v5s, with values equal to 78.6%, 77.8%, and 76%, respectively. However, YOLOv4-CSP showed the highest positive true rate, with a recall equal to 81.1%, while YOLOv3 presented the lowest rate, 64.4%, followed

**Table 2.** Optimized hyperparameters by “You Only Look Once” (YOLO) version.<sup>a</sup>

Hyperparameters	YOLOv3	YOLOv4	YOLOv5
Initial learning rate	0.01	0.00921	0.00351
Final learning rate	0.2	—	0.145
Stochastic gradient descent with momentum	0.937	0.939	0.93
Weight decay	0.0005	0.0005	0.00059
Warmup epochs	3.0	—	0.769
Warmup momentum	0.8	—	0.675
Warmup bias learning rate	0.1	—	0.124
Box	0.05	—	0.02
Cumulative layout shift loss fraction	0.5	0.459	0.375
Cumulative layout shift positive	1.0	0.982	0.92
Object loss gain weight	1.0	0.988	1.11
Object loss gain positive weight	1.0	1.05	0.509
Intersection over union threshold	0.2	0.2	0.2
Anchor threshold	4.0	3.99	2.0
Focal loss gamma	0.0	0.0	0.0
Image HSV hue augmentation	0.015	0.0146	0.0038
Image HSV saturation augmentation	0.7	0.712	0.436
Image HSV value augmentation	0.4	0.41	0.14
Image rotation	0.0	0.0	0.0
Image translation	0.1	0.486	0.0632
Image scale	0.5	0.498	0.212
Image shear	0.0	0.0	0.0
Image perspective	0.0	0.0	0.0
Image flip up to down	0.0	0.0	0.0
Image flip left to right	0.5	0.511	0.5
Mosaic	1.0	—	0.711
Image mix up	0.0	0.0	0.0
Generalized intersection over union	—	0.0471	—
Copy and paste	—	—	0
Anchor	—	—	3

<sup>a</sup>HSV, hue, saturation, value. A dash (—) indicates a hyperparameter not used by the YOLOv3, YOLOv4, and YOLOv5 models.

**Table 3.** Quality metrics (%) obtained in testing by “You Only Look Once” (YOLO) architectures.

Architecture	Precision	Recall	F1-score	@mAP.5	Accuracy
YOLOv3	78.6	64.4	70.8	62.2	51
YOLOv4-P5	65.2	76.4	70.4	71.1	79
YOLOv4-CSP	61.6	81.1	70.0	71.6	68
YOLOv5s	76.0	74.6	75.3	76.2	77
YOLOv5m	73.4	75.4	74.4	71.6	66
YOLOv5l	77.8	67.2	72.1	65.0	57

by YOLOv5l, with a recall of 67.2%. The rest of the YOLO architectures displayed a recall value above 75%. Therefore, the YOLOv5 models showed better precision and recall than the other architectures, which are summarized in the F1-score values. Among them, YOLOv5s achieved the highest F1-score value, equal to 75.3%, while YOLOv4-CSP achieved the lowest value, equal to 70.0%. In addition, YOLOv5s showed the highest @mAP.5 (76.2%), while YOLOv3 showed the lowest @mAP.5 (62.2%), followed by YOLOv5l (65%). All the other architectures obtained a value of 71%. Finally, YOLOv4-P5 and YOLOv5s showed similar accuracies in *P. rhoeas* detection, with values equal to 79% and 77%, respectively. However, YOLOv3 and YOLOv5l generated the worst results, with values equal to 51% and 57%, respectively. Thus, in terms of precision, recall, F1-score, @mAP.5, and accuracy, YOLOv5 achieved better results than YOLOv3 and YOLOv4. In addition, based on the F1-score and @mAP.5, YOLOv5s offered the best results, in agreement with Ayachi

**Table 4.** Comparative use of computing resources between “You Only Look Once” (YOLO) architectures.

Architecture	Training			Testing	
	Batch size	GPU memory %	Epoch per second	Inference GPU frames per second	Inference CPU frames per second
YOLOv3	32	68.8	50	42	1
YOLOv4-P5	32	83.8	78	28	0.2
YOLOv4-CSP	32	61	60	45	0.2
YOLOv5s	64	40	18	83	7
YOLOv5m	64	44.8	39	59	3
YOLOv5l	64	98.8	65	45	2

et al. (2020) and Wang and Yan (2021). Therefore, these results showed that the quality in the detection of *P. rhoeas* depends on both the architecture and the YOLO version selected.

Table 4 shows a comparison of the computational resources for training and testing used by the YOLO models evaluated. First, for the YOLOv3 and YOLOv4 architectures, it was necessary to consider a batch size equal to 32 versus 64 for YOLOv5 in the training phase, because in the former, the virtual machine was not able to finish the training process. Regarding the percentage of GPU memory usage, YOLOv5l was the most demanding, with a value equal to 98.8%. In contrast, YOLOv5s was the lowest, followed by YOLOv5m, with values of 40% and 44.8%, respectively. In addition, YOLOv4-P5 and YOLOv5l showed the highest number of epochs processed per second, 65 and 60, respectively, whereas, YOLOv5s achieved the lowest capacity, with only 18. From an inference point of view, YOLOv5s offered the highest FPS values analyzed using both GPU and CPU with a total of 83 and 7 frames, respectively. However, YOLOv4-P5s showed the least inference capacity, with values equal to 28 and 0.2. Therefore, YOLOv5s offered the best quality in the weed-detection process and the highest analytical capacity.

Figure 3 illustrates an example of the results of *P. rhoeas* detection in the testing phase using different YOLO architectures; weed plants are marked by bounding boxes with corresponding probabilities. These samples show how *P. rhoeas* detection can be successfully obtained in different real field situations, such as the presence or absence of crop plants, soil tonalities, or the presence of crop residues. The results changed according to the YOLO model assessed.

Weed control in winter cereals is usually carried out using a set of practices, such as plowing; maintenance of permanent soil covers and zero or minimum tillage (e.g., 25% soil disturbance); crop rotation (avoiding a monocrop system); use of pre- or post-emergence herbicides at the early crop and weed growth stage, alternating the kind of herbicide; and delaying the sowing date to allow weed emergence before crop emergence to increase the effect of herbicides. Regardless, *P. rhoeas* is a hard to control weed with evidence of herbicide-resistant biotypes due to incorrect agronomic praxis in many areas related to an inexistent crop rotation (mono-cereal crop systems) and a control tactic based on a single mix of postemergence herbicides without the diversification or alternation of herbicides from year to year that also helps to prevent nonresistant weeds becoming resistant.

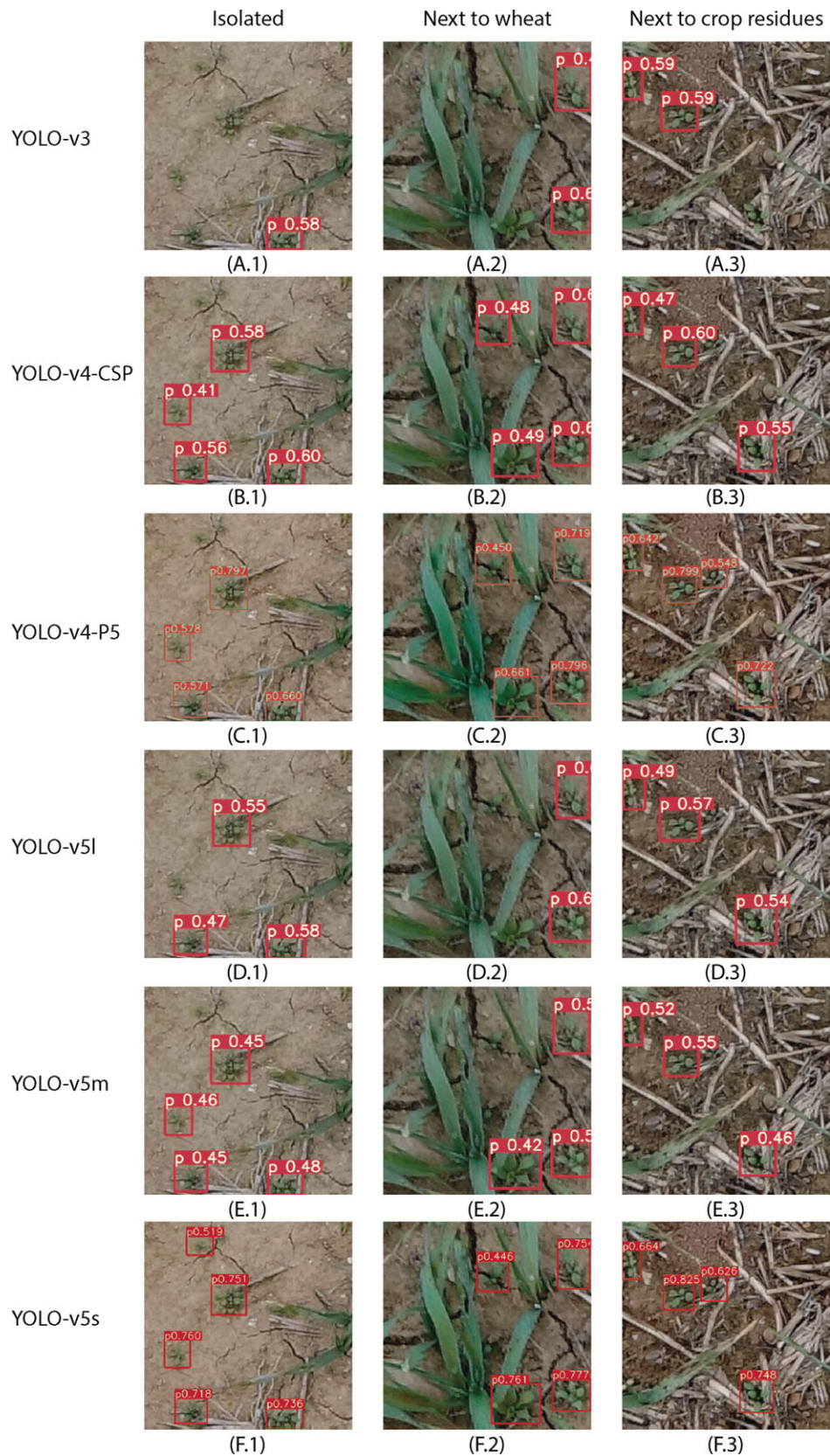


**Figure 3.** Examples of *Papaver rhoeas* detection in wheat using six YOLO models: (A) v3, (B) v4-CSP, (C) v4-P5, (D) v5l, (E) v5m, and (F) v5s. Different situations regarding *P. rhoeas* are also shown: (1) isolated, (2) next to wheat plants, and (3) next to crop residues.

To improve *P. rhoeas* control in wheat and based on the relevance of having timely and accurate weed maps at the seedling phase, a set of innovative, powerful, and efficient DL models focused on different YOLO architectures were studied. Table 3 shows all the quality metrics of the six object-detection models based on the YOLO architecture for locating and identifying young *P. rhoeas* plants in wheat. The results indicated that the use of YOLOv5s was suitable for the detection of *P. rhoeas* in the early season from on-ground imagery acquired in a wheat crop. The proposed DL model was able to detect approximately 75% of the *P. rhoeas* plants in the testing images, and approximately 75% of the detected objects were actual *P. rhoeas* plants. Previous works have used other DL models, such as VGGNet, GoogleNet, DetectNet, or Mask R-CNN (Mini et al. 2020; Peteinatos et al. 2020; Ying et al. 2021; Yu et al. 2019a, 2019b), to detect weeds with an accuracy ranging from 70% to 99%. The present work achieves the accuracy range of those works, but it must be noted that in the working scenario in most of those studies, the weed appears isolated from the crop and/or at an advanced stage of development, which simplifies the problem. For example, de Camargo et al. (2021) achieved precision and recall values of approximately 90% using the ResNet-18 model. However, *P. rhoeas* was in growth stages 17 to 19 on the BBCH scale (Meier 2001) with a range of 6 to 9 true leaves according to Pflanz et al. (2018), who used the same data set, while in the present work, *P. rhoeas* plants were in growth stages 12 to 14 of the BBCH scale with 2 to 4 true leaves. *Papaver rhoeas* plants at those growth stages are more difficult to detect, but it is a suitable period for herbicide application. Furthermore, although both references reported the use of UAV imagery, the good accuracy they achieved could also be related to the fact that they used imagery with higher spatial resolution (between 0.1 and 0.5 mm) than the images used in the present work (approximately 0.5 mm).

Focusing the discussion specifically on the use of different YOLO versions for weed detection, the present work has also achieved accuracies similar to those reached by other works. For example, modified models of YOLOv3 have been used for hedge bindweed [*Calystegia sepium* (L.) R. Br.] detection in sugar beet (*Beta vulgaris* L.) fields with a mAP around 0.80 (Gao et al. 2020); for weed detection in organic carrot (*Daucus carota* L. var. *sativus* Hoffm.) fields with an F1-score of 0.88 using input images with a relatively large size (832 by 832 pixels) (Czymbek et al. 2019); and for purslane (*Portulaca* spp.) detection with precision and recall of 71% and 78%, respectively (Partel et al. 2019). More recently, a modified version of YOLOv4 has been used for the detection of broadleaved and grass weeds (crabgrass [*Digitaria* spp.]; water plantain [*Alisma* spp.]; persicaria [*Polygonum* spp.]) in carrot fields, achieving a mAP of 87.80% (Ying et al. 2021).

The application of DL models in smart weeding technologies must consider both the accuracy of weed detection and the speed of inference. Of all the DL models, YOLO has been used in this work, because it is one of the fastest neural networks for real-time execution environments that do not have high-capacity hardware specifications (Kim et al. 2020). All the DL models evaluated in this work, with the exception of YOLOv4-P5, reached satisfactory inference speeds, allowing frame rates greater than 40 FPS when implemented on a GPU. Consequently, they could be studied for use in on-the-go *P. rhoeas* detection (e.g., in a robotic vehicle) by means of video cameras, as the standard frame rate for most off-the-shelf cameras is 30 FPS.

Our results are in the same range as previous works where smart herbicide sprayer and weed detection were used (Hussain et al.

2020; Partel et al. 2019). Thus, in our work, the DL model developed was based on object detection in such a way that the results obtained are suited to a smart herbicide sprayer being able to target individual weed plants using nozzles with narrow spray-distribution patterns. This would allow the implementation of SSWM strategies with the associated economic and environmental benefits and would follow the set of guidelines reported in European legislation addressing the sustainable use of pesticides (European Commission 2009, 2019), which are compatible with SSWM. According to these control tactics, object detection could also be appropriate for mechanical or alternative weed control using knives (Raja et al. 2020), laser beams (Marx et al. 2012), or flaming (Gonzalez-de-Santos et al. 2017). Once the detection model has been developed to detect *P. rhoeas*, future research should consider the development of a system that, by registering RGB videos in real time, detects the presence of *P. rhoeas* by a DL model such as the proposed one and sends a signal to a smart weeding implement. Thus, the variable-rate sprayer should include different RGB image sensors for capturing images, a computing unit for image processing, a microcontroller board to control the operations, several spray nozzles with valves, and a real-time kinematic GNSS receiver. Once images are acquired, detection models based on DL would be run by the computing unit. If a *P. rhoeas* plant were detected, its relative position would be calculated, and valves would be actuated to spray on the target. Simultaneously, its position would be registered by GNSS receiver to generate an infestation map.

In summary, a *P. rhoeas* detection model at an early stage was developed based on YOLO DL models (v3 to v5) through proximal RGB images taken in real wheat field conditions. To the best of the authors' knowledge, this is the first time that YOLOv5 has been proposed for weed seedling detection. This research was based on evaluating the quality of the models as well as the velocity and use of hardware resources in the detection process. The detection of *P. rhoeas* was carried out in a commercial plot with natural infestation (i.e., under uncontrolled situations), which reinforces the robustness obtained. Our results show that the quality and velocity of the detection varied according to the version of YOLO used, with YOLOv5s providing the best results. Therefore, the developed model can be integrated into a more complex scheme in which other systems, such as GNSS sensors, smart sprayers, or mechanical tools, should be involved. Such an integrated system would allow the generation of infestation maps or the real-time application of herbicides to improve the management of this hard to control weed.

**Acknowledgments.** This research was financed by project PID2020-113229RB-C44 (AEI/10.13039/501100011033) (Spanish MCIN funds). The authors thank J. Recasens, J. M. Peña, and A. I. de Castro for their help in field surveys. No conflicts of interest have been declared.

## References

- Andújar D, Weis M, Gerhards R (2012) An ultrasonic system for weed detection in cereal crops. *Sensors* 12:17343–17357
- Ayachi R, Afif M, Said Y, Atri M (2020) Traffic signs detection for real-world application of an advanced driving assisting system using deep learning. *Neural Process Lett* 51:837–851
- Bochkovskiy A, Wang C-Y, Liao H-YM (2020) YOLOv4: optimal speed and accuracy of object detection. arXiv:2004.10934
- Camargo T de, Schirrmann M, Landwehr N, Dammer K-H, Pflanz M (2021) Optimized deep learning model as a basis for fast UAV mapping of weed species in winter wheat crops. *Remote Sens* 13:1704

- Cirujeda A, Recasens J, Taberner A (2001) A qualitative quick-test for detection of herbicide resistance to tribenuron-methyl in *Papaver rhoeas*. *Weed Res* 41:523–534
- Cirujeda A, Recasens J, Taberner A (2006) Dormancy cycle and viability of buried seeds of *Papaver rhoeas*. *Weed Res* 46:327–334
- Cirujeda A, Recasens J, Torra J, Taberner A (2008) A germination study of herbicide-resistant field poppies in Spain. *Agron Sustain Dev* 28:207–220
- Czymmek V, Harders LO, Knoll FJ, Hussmann S (2019) Vision-based deep learning approach for real-time detection of weeds in organic farming. Pages 1–5 in 2019 IEEE International Instrumentation and Measurement Technology Conference (I2MTC). IEEE: Auckland, New Zealand. 10.1109/I2MTC.2019.8826921
- Dyrmann M, Karstoft H, Midtby HS (2016) Plant species classification using deep convolutional neural network. *Biosyst Eng* 151:72–80
- European Commission (2009) Directive 2009/128/EC of the European Parliament and of the Council of 21 October 2009 establishing a framework for community action to achieve the sustainable use of pesticides (text with EEA relevance). 16 p. <https://eur-lex.europa.eu/LexUriServ/LexUriServ.do?uri=OJ:L:2009:309:0071:0086:en:PDF>. Accessed: December 21, 2022
- European Commission (2019) Directive 2019/782/EU of 15 May 2019 amending Directive 2009/128/EC of the European Parliament and of the Council as regards the establishment of harmonised risk indicators. 7 p. <https://eur-lex.europa.eu/legal-content/EN/TXT/HTML/?uri=CELEX:32019L0782&from=EN>. Accessed: December 21, 2022
- Fernández-Quintanilla C, Dorado J, Andújar D, Peña JM (2020) Site-specific based models. Pages 143–157 in Chantre GR, González-Andújar JL, eds. *Decision Support Systems for Weed Management*. Cham, Switzerland: Springer Nature
- Fernández-Quintanilla C, Peña JM, Andújar D, Dorado J, Ribeiro A, López-Granados F (2018) Is the current state of the art of weed monitoring suitable for site-specific weed management in arable crops? *Weed Res* 58:259–272
- Gao J, French AP, Pound MP, He Y, Pridmore TP, Pieters JG (2020) Deep convolutional neural networks for image-based *Convolvulus sepium* detection in sugar beet fields. *Plant Methods* 16:29
- Gómez-Candón D, De Castro AI, López-Granados F (2014) Assessing the accuracy of mosaics from unmanned aerial vehicle (UAV) imagery for precision agriculture purposes in wheat. *Precis Agric* 15:44–56
- Gonzalez-de-Santos P, Ribeiro A, Fernandez-Quintanilla C, Lopez-Granados F, Brandstötter M, Tomic S, Pedrazzi S, Peruzzi A, Pajares G, Kaplanis G, Perez-Ruiz M, Valero C, del Cerro J, Vieri M, Rabatel G, Debilde B (2017) Fleets of robots for environmentally-safe pest control in agriculture. *Precis Agric* 18:574–614
- Hasan ASMM, Sohail F, Diepeveen D, Laga H, Jones MGK (2021) A survey of deep learning techniques for weed detection from images. *Comput Electron Agric* 184:106067
- Heijting S, Van Der Werf W, Stein A, Kropff MJ (2007) Are weed patches stable in location? Application of an explicitly two-dimensional methodology. *Weed Res* 47:381–395
- Hemming J, Rath T (2002) Image processing for plant determination using the Hough transform and clustering methods. *Gartenbauwissenschaft* 67:1–10
- Holm L, Doll J, Holm E, Pancho J V, Herberger JP (1997) *Papaver rhoeas*. Pages 555–561 in *World Weeds: Natural Histories and Distribution*. New York: Wiley
- Hussain N, Farooque AA, Schumann AW, McKenzie-Gopsill A, Esau T, Abbas F, Acharya B, Zaman Q (2020) Design and development of a smart variable rate sprayer using deep learning. *Remote Sens* 2:4091
- Izquierdo J, Blanco-Moreno JM, Chamorro L, Recasens J, Sans FX (2009) Spatial distribution and temporal stability of prostrate knotweed (*Polygonum aviculare*) and corn poppy (*Papaver rhoeas*) seed bank in a cereal field. *Weed Sci* 57:505–511
- Izquierdo J, Milne AE, Recasens J, Royo-Esnal A, Torra J, Webster R, Baraibar B (2020) Spatial and temporal stability of weed patches in cereal fields under direct drilling and harrow tillage. *Agronomy* 10:452
- Jiang P, Ergu D, Liu F, Cai Y, Ma B (2022) A review of yolo algorithm developments. *Procedia Comp Sci* 199:1066–1073
- Jiménez-Brenes FM, López-Granados F, Torres-Sánchez J, Peña JM, Ramírez P, Castillejo-González IL, de Castro AI (2019) Automatic UAV-based detection of *Cynodon dactylon* for site-specific vineyard management. *PLoS ONE* 14: e0218132
- Jun X, Sun Y, Che J, Bagavathiannan M, Yu J, Chen, Y (2022) A novel deep learning-based method for detection of weeds in vegetables. *Pest Manag Sci* 78:1861–1869
- Jocher G, Stoken A, Borovec J, NanoCode012, ChristopherSTAN, Changyu L, Laughing, Hogan A, lorenzomamma, tkianai, yxNONG, AlexWang1900, Diaconu L, Marc, Wanghaoyang0106, et al. (2020) ultralytics/yolov5: v3.0. Zenodo. <https://doi.org/10.5281/zenodo.3983579>. Accessed: September 30, 2020
- Jurado-Expósito M, López-Granados F, García-Torres L, García-Ferrer A, Orden MS de la, Atenciano S (2003) Multi-species weed spatial variability and site-specific management maps in cultivated sunflower. *Weed Sci* 51:319–328
- Kazmi W, Garcia-Ruiz FJ, Nielsen J, Rasmussen J, Andersen HJ (2015) Detecting creeping thistle in sugar beet fields using vegetation indices. *Comput Electron Agric* 112:10–19
- Khan S, Tufail M, Khan MT, Khan ZA, Anwar S (2021) Deep learning-based identification system of weeds and crops in strawberry and pea fields for a precision agriculture sprayer. *Precis Agric* 22:1711–1727
- Kim J, Sung J-Y, Park S (2020) Comparison of faster-RCNN, YOLO, and SSD for real-time vehicle type recognition. Pages 1–4 in 2020 IEEE International Conference on Consumer Electronics—Asia (ICCE-Asia). Seoul, South Korea: Institute of Electrical and Electronics Engineers
- López-Granados F (2011) Weed detection for site-specific weed management: mapping and real-time approaches. *Weed Res* 51:1–11
- López-Granados F, Torres-Sánchez J, De Castro A-I, Serrano-Pérez A, Mesas-Carrascosa FJ, Peña JM (2016) Object-based early monitoring of a grass weed in a grass crop using high resolution UAV imagery. *Agron Sustain Dev* 36:67
- Marx C, Barcikowski S, Hustedt M, Haferkamp H, Rath T (2012) Design and application of a weed damage model for laser-based weed control. *Biosyst Eng* 113:148–157
- Meier U (2001) Growth Stages of Mono- and Dicotyledonous Plants. BB Monograph. Federal Biological Research Centre for Agriculture and Forestry. <https://www.politicheagricole.it/flex/AppData/WebLive/Agrometeo/MIIEPFY800/BBCHEng2001.pdf>. Accessed: April 14, 2021
- Mesas-Carrascosa FJ, Torres-Sánchez J, Clavero-Rumbao I, García-Ferrer A, Peña JM, Borra-Serrano I, López-Granados F (2015) Assessing optimal flight parameters for generating accurate multispectral orthomosaics by UAV to support site-specific crop management. *Remote Sens* 7:12793–12814
- Meyer G, Mehta T, Kocher M, Mortensen D, Samal A (1998) Textural imaging and discriminant analysis for distinguishing weeds for spot spraying. *Trans ASAE* 41(4):1189
- Mini GA, Sales DO, Luppe M (2020) Weed segmentation in sugarcane crops using Mask R-CNN through aerial images. Pages 485–491 in 2020 International Conference on Computational Science and Computational Intelligence (CSCI). Las Vegas, NV: American Council on Science and Education
- Mulla DJ (2013) Twenty five years of remote sensing in precision agriculture: key advances and remaining knowledge gaps. *Biosyst Eng* 114:358–371
- Oh S, Chang A, Ashapure A, Jung J, Dube N, Maeda M, Gonzalez D, Landivar J (2020) Plant counting of cotton from UAS imagery using deep learning-based object detection framework. *Remote Sens* 12:2981
- OpenCV (2021) Home page. <https://opencv.org>. Accessed: April 21, 2021
- Oppenheim D, Shani G, Erlich O, Tsrur L (2019) Using deep learning for image-based potato tuber disease detection. *Phytopathology* 109:1083–1087
- Partel V, Charan Kakarla S, Ampatzidis Y (2019) Development and evaluation of a low-cost and smart technology for precision weed management utilizing artificial intelligence. *Comput Electron Agric* 157:339–350
- Peña JM, Torres-Sánchez J, Serrano-Pérez A, de Castro AI, López-Granados F (2015) Quantifying efficacy and limits of unmanned aerial vehicle (UAV) technology for weed seedling detection as affected by sensor resolution. *Sensors* 15:5609–5626
- Peña-Barragán JM, de Castro AI, Torres-Sánchez J, Jiménez-Brenes FM, Valencia F, López Granados F (2017) Principales variables para la detección de plántulas de amapola (*Papaver rhoeas*) en imágenes tomadas con un vehículo aéreo no tripulado. Pages 425–430 in XVI Congreso de la Sociedad Española de Malherbología. Pamplona: Universidad Pública de Navarra

- Pérez AJ, López F, Benlloch JV, Christensen S (2000) Colour and shape analysis techniques for weed detection in cereal fields. *Comput Electron Agric* 25:197–212
- Perez L, Wang J (2017) The effectiveness of data augmentation in image classification using deep learning. arXiv:1712.04621
- Pérez-Ortiz M, Peña JM, Gutiérrez PA, Torres-Sánchez J, Hervás-Martínez C, López-Granados F (2016) Selecting patterns and features for between- and within- crop-row weed mapping using UAV-imagery. *Expert Syst Appl* 47:85–94
- Peteinatos GG, Reichel P, Karouta J, Andújar D, Gerhards R (2020) Weed identification in maize, sunflower, and potatoes with the aid of convolutional neural networks. *Remote Sens* 12:4185
- Peteinatos GG, Weis M, Andújar D, Rueda Ayala V, Gerhards R (2014) Potential use of ground-based sensor technologies for weed detection. *Pest Manag Sci* 70:190–199
- Pflanz M, Nordmeyer H, Schirrmann M (2018) Weed mapping with UAS imagery and a bag of visual words based image classifier. *Remote Sens* 10:1530
- Raja R, Nguyen TT, Slaughter DC, Fennimore SA (2020) Real-time robotic weed knife control system for tomato and lettuce based on geometric appearance of plant labels. *Biosyst Eng* 194:152–164
- Redmon J, Divvala S, Girshick R, Farhadi A (2016) You Only Look Once: unified, real-time object detection. Pages 779–788 in *Proceedings of the IEEE Conference on Computer Vision and Pattern Recognition (CVPR)*. Las Vegas, NV: Institute of Electrical and Electronics Engineers
- Redmon J, Farhadi A (2018) YOLOv3: an incremental improvement. arXiv:1804.02767
- Saavedra M, García-Torres L, Hernández-Bermejo E, Hidalgo B (1989) Weed flora in the Middle Valley of the Guadalquivir, Spain. *Weed Res* 29:167–179
- Santos Ferreira A dos, Freitas DM, da Silva GG, Pistori H, Folhes MT (2019) Unsupervised deep learning and semi-automatic data labeling in weed discrimination. *Comput Electron Agric* 165:104963
- Sharpe SM, Schumann AW, Boyd NS (2020) Goosegrass detection in strawberry and tomato using a convolutional neural network. *Sci Rep* 10(1):1–8
- Shorewala S, Ashfaq A, Sidharth R, Verma U (2021) Weed density and distribution estimation for precision agriculture using semi-supervised learning. *IEEE Access* 9:27971–27986.
- Su D, Qiao Y, Kong H, Sukkarieh S (2021) Real time detection of inter-row ryegrass in wheat farms using deep learning. *Biosyst Eng* 204: 198–211
- Tellaache A, Pajares G, Burgos-Artizzu XP, Ribeiro A (2011) A computer vision approach for weeds identification through support vector machines. *Appl Soft Comput* 11:908–915
- Thuan D (2021) Evolution of Yolo Algorithm and Yolov5: The State-of-the-Art Object Detection Algorithm. Bachelor's thesis. Oulu University of Applied Sciences, Finland. 61 p
- Tong K, Wu Y, Zhou F. (2020). Recent advances in small object detection based on deep learning: a review. *Image Vis Comput* 97:103910
- Torra J, Cirujeda A, Taberner A, Recasens J (2010) Evaluation of herbicides to manage herbicide-resistant corn poppy (*Papaver rhoeas*) in winter cereals. *Crop Prot* 29:731–736
- Torra J, Gonzáles-Andújar JL, Recasens J (2008) Modelling the population dynamics of *Papaver rhoeas* under various weed management systems in a Mediterranean climate. *Weed Res* 48:136–146
- Torra J, Recasens J (2008) Demography of corn poppy (*Papaver rhoeas*) in relation to emergence time and crop competition. *Weed Sci* 56:826–833
- Torres-Sánchez J, López-Granados F, Peña JM (2015) An automatic object-based method for optimal thresholding in UAV images: application for vegetation detection in herbaceous crops. *Comput Electron Agric* 114:43–52
- Torres-Sánchez J, Peña JM, de Castro AI, López-Granados F (2014) Multi-temporal mapping of the vegetation fraction in early-season wheat fields using images from UAV. *Comput Electron Agric* 103:104–113
- Wang C-Y, Liao H-YM, Wu Y-H, Chen P-Y, Hsieh J-W, Yeh I-H (2020) CSPNet: a new backbone that can enhance learning capability of CNN. Pages 390–391 in *Proceedings of the IEEE/CVF conference on computer vision and pattern recognition workshops*. Seattle, WA: Computer Vision Foundation
- Wang L, Yan WQ (2021) Tree leaves detection based on deep learning. Pages 26–38 in Nguyen, M, Yan, W-Q, Ho, H, eds. *Geometry and Vision: First International Symposium*. Auckland, New Zealand: ISGV
- Wilson BJ, Wright KJ, Brain P, Clements M, Stephens E (1995) Predicting the competitive effects of weed and crop density on weed biomass, weed seed production and crop yield in wheat. *Weed Res* 35:265–278
- Woebbecke D, Meyer G, Von Bargaen K, Mortensen D (1995) Shape features for identifying young weeds using image analysis. *Trans ASAE* 38(1):271–281
- Ying B, Xu Y, Zhang S, Shi Y, Liu L (2021) Weed detection in images of carrot fields based on improved YOLO v4. *Traitement du Signal* 38:341–348
- Yu J, Schumann AW, Cao Z, Sharpe SM, Boyd NS (2019a) Weed detection in perennial ryegrass with deep learning convolutional neural network. *Frontiers in Plant Sci* 10:1422
- Yu J, Sharpe SM, Schumann AW, Boyd NS (2019b) Deep learning for image-based weed detection in turfgrass. *Eur J Agron* 104:78–84